Available online at www.sciencedirect.com
SCIENCE DIRECT
Biochimica et Biophysica Acta 1712 (2005) 37 – 51
BIOCHIMICA ET BIOPHYSICA ACTA
BBA
http://www.elsevier.com/locate/bba

Self-association of glutamic acid-rich fusion peptide analogs of influenza hemagglutinin in the membrane-mimic environments: Effects of positional difference of glutamic acids on side chain ionization constant and intra- and inter-peptide interactions deduced from NMR and gel electrophoresis measurements

Ding-Kwo Chang*, Shu-Fang Cheng, Chi-Hui Lin, Eric Assen B. Kantchev, Cheng-Wei Wu

Institute of Chemistry, Academia Sinica, Taipei, Taiwan, Republic of China

Received 21 December 2004; received in revised form 14 March 2005; accepted 5 April 2005
Available online 28 April 2005

Abstract

Two glutamic acid-rich fusion peptide analogs of influenza hemagglutinin were synthesized to study the organization of the charged peptides in the membranous media. Fluorescence and gel electrophoresis experiments suggested a loose association between the monomers in the vesicles. A model was built which showed that a positional difference of 3, 7 and 4, 8 results in the exposure of Glu3 and Glu7 side chains to the apolar lipidic core. Supportive results include: first, pK_a values of two pH units higher than reference value in aqueous medium for Glu3 and Glu7 CγH, whereas the deviation of pK_a from the reference value for Glu4 and Glu8 CγH is substantially smaller; second, Hill coefficients of titration shift of these protons indicate anti-cooperativity for Glu3 and Glu7 side chain protons but less so for Glu4 and Glu8, implying a strong electrostatic interaction between Glu3 and Glu7 possibly resulting from their localization in an apolar environment; third, positive and larger titration shift for NH of Glu3 is observed compared to that of Glu4, suggesting stronger hydrogen bond between the NH and the carboxylic group of Glu3 than that of Glu4, consistent with higher degree of exposure to hydrophobic medium for the side chain of Glu3.
© 2005 Elsevier B.V. All rights reserved.

Keywords: Charged residue; Membrane insertion; Hydrogen bond; Rhodamine self-quenching; Fluorescence resonance energy transfer; Self-assembly; Proton titration shift; Ionization constant shift

1. Introduction

The entry of enveloped viruses into target cells is mediated by their fusion proteins, which are transformed into the fusogenic state by binding to cellular receptors, e.g., HIV-1 or low pH in the endosome after endocytosis, e.g., influenza virus. Since viral nucleocapsid, a macromolecular complex, is translocated from the viral to the cellular compartment, the membrane fusion is thought to be orchestrated by the cooperation of several fusion protein molecules to form sufficiently large fusion pores. The concept has been invoked in numerous models for viral fusion mechanism [1,2] and supported by experimental observations [3–6]. On the other hand, it has also been reported that the inhibitory function of phospholamban was activated by the depolymerization of the protein molecules [7]. Val-to-Glu mutation in the transmembrane segment of the neu/erbB-2 receptor is suggested to enhance dimerization of the receptor, resulting in the activation of signal transduction [8]. The self-assembly of protein segments is therefore essential for the protein to exert its function.

For the fusion protein of influenza virus HA2, its N-terminal fusion peptide of ~20 amino acid residues has been

* Corresponding author. Tel.: +886 2 27898594; fax: +886 2 27831237.
E-mail address: dkc@chem.sinica.edu.tw (D.-K. Chang).

0005-2736/$ - see front matter © 2005 Elsevier B.V. All rights reserved.
doi:10.1016/j.bbamem.2005.04.003

shown to insert into membrane bilayer [9]. Similar to other class I viruses, the HA2 fusion peptide undergoes conformational change, notably helix enhancement, upon binding to lipid bilayer; however, the helical structure is distorted and less stable for the C-terminal portion. Additionally, an oblique insertion angle appeared to correlate with fusion activity. A loose association in the membrane of a 25-mer HA2 fusion peptide fragment was deduced from a fluorescence self-quenching experiment. Interestingly, there are three acidic residues at positions 11, 15 and 19 in the fusion peptide sequence amidst otherwise highly hydrophobic residues. These acidic residues are protonated at the fusogenic pH. It has also been suggested that the region 1–15 of the fusion peptide is embedded in the apolar milieu of the membrane [10]. In an attempt to increase the solubility of the fusion peptide in aqueous medium, glutamic acid was substituted for glycine at positions 4 and 8, and aspartic acid at position 19 [11–13]. In addition, an analog in which positions 3 and 7 were replaced with glutamic acid was also studied (designated E5(3,7)). The membrane affinity and fusion activity were not significantly affected. However, it is uncertain that the substituted residues are still in the nonpolar domain of the membrane, considering, in particular, that the side chains of glutamic acid residues at positions 3, 7, 4 and 8 are ionized at neutral pH. In a previous communication, we found increased pH sensitivity of fusion activity of E5 analogs in comparison with the wild type fusion peptide. Furthermore, alteration in the fusion activity along with the secondary structure with pH change is more pronounced in the N-terminal half of the fusion peptide analogs. These findings prompted us to further examine the self-assembly of E5 analogs in the bilayer, in view of the additional acidic residues and their positions relative to the rest of the peptides and the effect on fusion activity. The five glutamic acids can be used to study the hydrogen bond, side chain interaction in conjunction with the structure information by NMR spectroscopy from pK_a values and pH titration profile of ^{1}H chemical shift [14,15]. In the following, these parameters are used to deduce the relative orientation of the peptide monomers in the trimer.

In addition, to shed some light on the fusion mechanism, the present study on the Glu-rich peptides may provide more insight into the interaction of a charged residue with lipid and with other peptide within the hydrocarbon region of the membrane. Thus, electrostatic interaction as well as hydrogen bonding in membrane may be critical in conferring the stability of transmembrane protein assembly and folding, thereby influencing the biosynthesis process [16] and membrane protein function. Remarkably, self-association of the peptides investigated is retained at neutral pH in the membranous medium revealed in the gel electrophoresis, fluorescence self-quenching and fluorescence resonance energy transfer (FRET) data; hence, we inferred that water molecules mediate charge–charge interaction and that tight self-association is not required for fusion activity for the fusion peptides. We also noted that the position of the charge residues has a discernible effect on the self-association of the peptide molecules in the membranous medium and the difference in the insertion depth of the N-terminal region between the two E5 analogs [17]; both results are explained with the proposed trimeric model.

A comparison of the charge–charge interaction in low (membrane interior) and high (aqueous) dielectric media also affords more information on the protein folding in these environments, for which the electrostatic force is an important factor. As an example of the relevance of negative charge residues to the protein structure and function, Glu118, Glu120 and Arg117 in the C-terminal region of *KcsA* potassium channel have been implicated in the stabilization of the tetramer and for pH sensing of the protein [18]. Electrostatic interaction between charged residues in the transmembrane domain has been found to be essential in the organization of the T-cell receptor–CD3 complex [19]. Ionic interaction is also critical to the quaternary structure of the proteins; for example, a Glu-to-Val mutation in the β-chain of hemoglobin results in the aggregation and filament formation of the red blood cell. An analysis of our results may thus provide more insight into the mechanism underlying the signal transmission through membrane and ion channels [20] as well as the interactions between the ligands and side chain groups of transporter proteins.

2. Materials and methods

2.1. Materials

The 1,2-dimyristoyl-*sn*-glycero-3-phosphocholine (DMPC) and 1,2-dimyristoyl *sn*-glycero-3-phosphoglycerol (DMPG) used in this work were obtained from Avanti Polar Lipids (Alabaster, AL, USA). 5(6)-Carboxytetramethylrhodamine hydrochloride (TAMRA) was purchased from Molecular Probes, Inc. (MPI, Eugene, Oregon). 4-Chloro-7-nitrobenz-2-oxa-1,3-diazole (NBD-Cl) was purchased from Sigma (St. Louis, MO, USA). The synthesis, purification and characterization of the peptides used were described previously [17]. Briefly, the peptides corresponding to residues 1–25 of HA2, HA2(1–25), NH_2-GLFGAIAGFIENGWEGMIDGWYGFR-COOH (strain X31) of the influenza virus, and its two E5 variants, E5(4,8) and E5(3,7) (with Glu substitution at position 19 and positions 4, 8 and 3, 7, respectively), were assembled by Fmoc/*t*-Bu solid phase peptide synthesis using a peptide synthesizer (Protein Technologies, Tucson, AZ, USA, model Rainin PS3). All chemicals and solvents were used without further purification. The N-terminal free peptides were labeled with TAMRA using the standard Fmoc–amino acid coupling protocol with 12-h coupling time. NBD was labeled according to the procedure of Rapaport and Shai [21] with modifications. Briefly, the N-terminal free peptide resin was

suspended in DMF, and *N,N*-diisopropyl-*N*-ethylamine was added (35-fold excess), followed by the drop-wise addition of NBD-Cl (30-fold excess) dissolved in a small volume of DMF for 5 h. The crude peptides were purified on a Hewlett-Packard 1100 HPLC system with a semi-preparative Vydac C-18 column. The purified peptides were lyophilized and their sequence and purity were ascertained by ESI MS.

2.2. Fluorescence experiments

2.2.1. Cobalt quenching on NBD-labeled HA2(1–25) and E5 analogs

The Co^{2+} quenching experiments were performed on a Hitachi F-2500 Fluorescence Spectrophotometer equipped with a thermostated cell holder with a stirrer at 37 °C. Using 1-cm^2 semi-micro quartz cuvettes, spectra in 500–650 nm range were collected by employing 467-nm excitation wavelength with a scan rate of 300 nm/min for wavelength scan and 530 nm emission wavelength for time scan. The response time was set at 0.4 s, and slit bandwidths for excitation and emission were 10 nm. The NBD-labeled peptide was suspended in DMPC:DMPG 1:1 vesicular solution (150:150 μM) or 50% ethanol at pH 5.0 or pH 7.4 (PB buffer) and measurements were taken until the fluorescence signal attained a steady value. The final concentrations of the peptide were 0.06 μM. An incremental amount of $CoCl_2$ stock solution (0.1 M) was then injected into the cuvette to give final concentrations in the range of 0.02 to 2.0 mM. Corrections due to dilution were made to the observed fluorescence intensities. The data were analyzed using the Stern–Volmer equation:

$$F_0/F = 1 + K_{SV}[Q]$$

where F_0 and F are, respectively, the intensity of NBD fluorescence before and after adding a given amount of $CoCl_2$ solution, $[Q]$ is the concentration of the quencher and the slope K_{SV} is the Stern–Volmer constant.

2.2.2. Self-association monitored by self-quenching of the Rho-labeled peptides

To estimate the self-association between adjacent HA2 trimers, the variation of Rho-labeled/unlabeled HA2 25-mer composition experiments were performed on a Jasco spectrofluorometer, model FP-777, using a 1 cm^2 semi-micro quartz cuvette with stirrer. 20 μl of the different compositions of labeled and unlabeled peptides was added to 980 μl DMPC:DMPG 1:1 in phosphate buffer at pH 7.4 and 5.0. The total (labeled plus unlabeled) peptide concentration was kept constant at 1 μM while the fraction of the labeled peptide, x, was varied from 0.05 to 1 in DMPC:DMPG (100 μM:100 μM) vesicular suspension. The normalized emission intensity I_x/x was plotted against x [6]. To monitor the rhodamine fluorophore, the excitation and emission wavelengths were set at 530 and 578 nm, respectively. The mixture was stirred at 37 °C until a steady value was achieved and read off. Spectra were recorded from 500 to 650 nm using an excitation wavelength of 530 nm. The slit bandwidths for excitation and emission were 5 nm and 1.5 nm, respectively. A scan rate of 200 nm/min was used for the wavelength scans with the response time of 1 s.

2.2.3. Resonance energy transfer efficiency between NBD- and Rho-labeled peptides

FRET experiments between NBD (donor) and Rho (acceptor) were carried out on a Hitachi F-2500 Fluorescence Spectrophotometer. All parameters were the same as described in Section 2.2.1. NBD-labeled/unlabeled peptide mixture in DMPC:DMPG (1:1) was used as starting solution, to which was added the Rho-labeled/NBD-labeled peptide mixture in DMPC:DMPG (1:1). Titration experiments proceeded with a stepwise decrease of the former sample and increase of the latter to keep constant the concentrations of NBD-labeled peptide, total (labeled and unlabeled) peptide and lipid. The final concentrations of total peptide and DMPC:DMPG were 0.12 μM and 150:150 μM, respectively. Appropriate blanks were subtracted to obtain the corrected spectra. The percentage transfer efficiency (E) was calculated by:

$$E = (1 - I_{da}/I_a) \times 100\%$$

where I_{da} and I_d are the fluorescence intensities of the donor with and without the acceptor, respectively. For comparison, E values obtained from the random distribution of donors and acceptors in the membrane was shown using a Förster distance (R_0) of 50 Å for the pair [22,23].

2.3. Perfluorooctanoic acid-polyacrylamide gel electrophoresis (PFO-PAGE)

To better detect the oligomerization of HA2(1–25) and its two E5 variants, electrophoresis was performed with a mild detergent, perfluorooctanoic acid (PFO). A continuous gel was prepared using acrylamide (18.3% T) containing *N,N′*-methylenebisacrylamide (2.67% C) in the pH 7.4 buffer (0.1% PFO, 43 mM imidazole, and 35 mM HEPES). Approximately 0.1% ammonium persulfate and 0.05% tetramethylenediamine were mixed with the acrylamide solution immediately before casting the gel. Peptides were dissolved in 1,1,1,3,3,3-hexafluoro-2-propanol and mixed with the ethanol-solubilized lysolipid, 1-dodecanoyl-*sn*-glycero-3-phosphocholine (lysoPC). After removing the organic solvents by nitrogen flow, the peptide–lysolipid mixture was resuspended in 43 mM imidazole–35 mM HEPES buffer (pH 7.4) or 80 mM γ-aminobutyric acid/20 mM acetic acid buffer (pH 4.8). The concentrations of the peptide and the lysoPC were ~0.5 and 3 mM, respectively. An equal volume of the neutral (43 mM imidazole, 35 mM HEPES, 4% PFO, 40% glycerol, 0.01% bromophenol blue, adjusted to pH 7.4 by 1 N NaOH) or the acidic loading buffer (80 mM γ-aminobutyric acid, 20 mM acetic acid, 2%

PFO, 40% glycerol, 0.01% bromophenol blue, adjusted to pH 4.8 by 1 N NaOH) was then mixed with the peptide–lysolipid suspension of the same pH. An aliquot of 15 μl of the dissolved mixture was loaded into the gel, and the electrophoresis was conducted at 20 mA constant current for 90 min, followed by silver staining (GelCode SilverSNAP stain kit II, Pierce Co., USA).

2.4. NMR experiments

Micellar suspension containing d^{25}-SDS and each of the 25-mer fusion peptide analogs (100:1.0 mM) were used for one-dimensional and two-dimensional ^{1}H NOESY and TOCSY NMR experiments performed on a Bruker AMX-500 spectrometer at 298 K, as described previously [24].

Proton chemical shift titration data were fitted to Eq. (1) with a software package written by H. W. Anthonson (www.nmrfam.wisc.edu/~hwa).

$$\delta_{\mathrm{obs}} = \delta_B + \Delta\delta \times 10^{n(pK_a - \mathrm{pH})}/(1 + 10^{n(pK_a - \mathrm{pH})}) \quad (1)$$

where δ_{obs}, δ_{B}, $\Delta\delta$ and n are the observed, unprotonated and titration chemical shifts, and Hill coefficient, respectively.

3. Results

3.1. Models for the trimers of HA2(1–25), E5(4,8) and E5(3,7) helices suggest positions 3, 7 on the exterior face of the trimer

Fig. 1A–C illustrate the amphipathicity of the fusion peptide of influenza virus HA2(1–25), E5(4,8) and E5(3,7) as well as the model for the trimeric organization, using helix wheel representation. It is noted that positions 4, 8, 11, 15 and 19 are on the polar face orienting toward one another while the nonploar residues are on the external face in the trimer, as observed in some integral membrane proteins for which the lipid-facing residues were found more hydrophobic than those in the interior [25]. As will be clear in the following presentation, this orientation, for which the polar or charged residues are sequestered in the interior of the trimer, is consistent with the results on the self-assembly and proton NMR chemical shift titration of the fusion peptides in the membranous milieu. Furthermore, glycine has been implicated in the assembly of transmembrane helix association [26,27]. The architecture of the oligomeric packing for these peptides is similar to the porin trimer in terms of distribution of polar residues in the trimer interface and nonpolar residues around the trimer circumference [28]. We

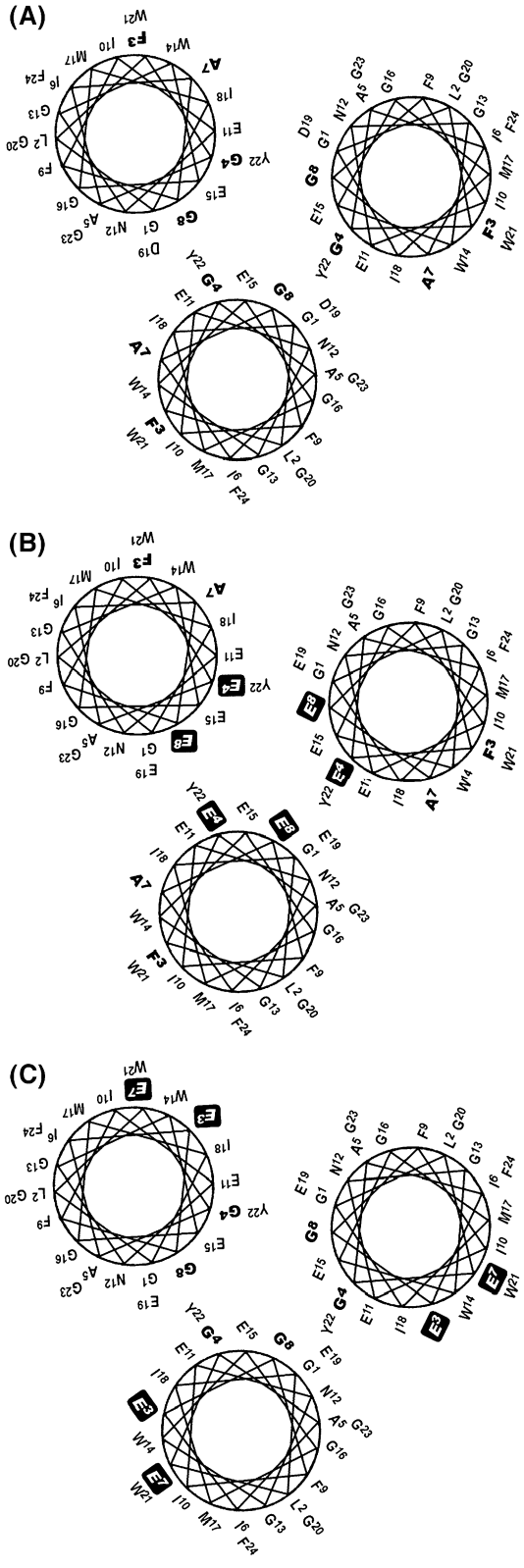

Fig. 1. Trimeric assembly model for HA2(1–25), E5(4,8) and E5(3,7) in the membrane with emphasis on the relative orientation of the monomers. Note that Glu as well as Gly residues are sequestered on the face away from membrane hydrocarbon core. Also, the difference in the position of the N-terminal Glu residues for the two Glu-rich variants, when their N-terminal portion is embedded in the apolar core of membrane, results in a higher extent of exposure of Glu3 and Glu7 to the hydrophobic milieu than Glu4 and Glu8.

will provide experimental evidence for the proposed orientation from comparison of the E5 analogs in the following results. We also note that the arguments on the architecture and membrane interaction using the trimeric model are also valid for the tetrameric or pentameric model.

3.2. Cobalt quenching of NBD fluorescence for the labeled fusion peptides in DMPC:DMPG vesicle and ethanol solution at pH 5.0 and 7.4 reveals a near-surface localization for the N-terminus of the peptides at neutral pH

To examine the pH dependence of the penetration of the peptide variants into the membrane, we monitored the quenching of N-terminally labeled NBD by Co^{2+}. Fig. 2A illustrates NBD emission as a function of wavelength for HA2(1–25) and the two E5 variants in DMPC:DMPG vesicular dispersion and in aqueous solution. A substantial increase in the fluorescence and blue shift is observed for NBD labeled to the three peptides, indicating that the N-terminal region of the fusion peptides is near the hydrophobic membrane core. In Fig. 2B, K_{SV} (Stern–Volmer constant) values obtained in 1:1 ethanol:water (v/v) solution was used as reference for the surface quenching of NBD by Co^{2+}. The figure summarizes K_{SV} of the three fusion peptide analogs in the vesicle and in ethanol solution at both acidic and neutral pH. Remarkably, at pH 7.4, K_{SV} values are close in the two media for all the three peptides tested; by contrast, at pH 5.0, K_{SV} values are substantially smaller in the vesicular dispersion than in the ethanol solution for the peptide analogs. The results reaffirm that the N-terminus of the peptides is located near the surface of the vesicle at neutral pH, but inserts more deeply into the interior of the vesicle at acidic pH, consistent with the trend in intensity observed with the two pHs for the three peptide analogs in Fig. 2A.

The data of Fig. 2A and B show that the parent peptide penetrates more deeply, followed by E5(4,8) and E5(3,7), under the same pH. As will be discussed in the next section, the difference in intensity and K_{SV} monitored by NBD likely reflects the effect of the position of substituted Glu residues on the topology of the peptide in the membrane [29].

3.3. Self-association of the fusion peptide analogs is demonstrated by self-quenching of fluorescence of rhodamine and by FRET between the NBD and rhodamine fluorophores attached to the E5 peptides

To determine the self-association of the fusion peptides in the membrane, rhodamine (Rho) labeled peptides were mixed with unlabeled peptide in a gradually increasing ratio, keeping the total concentration constant. The normalized fluorescence intensity is plotted against $1-x$ where x is the fraction of labeled peptide in Fig. 3A. In the high labeling regime, the result mainly reflects intra-trimer association, whereas the low labeling region emphasizes inter-trimer interaction. The data therefore indicate the intra-trimer association is strongest for HA2(1–25), followed by E5(3,7) and E5(4,8), at both pH levels tested. It is of interest that there is virtually no difference in the extent of intra-trimer interaction between pH 5.0 and 7.4 for the wild type peptide while the association is tighter at acidic pH for the two E5 analogs. This suggests that the protonation results in more stable trimers due to reduced electrostatic repulsion between the side chains of glutamic acid residues on the peptides (cf. Fig. 1). In support of the orientation given in the model, the tighter packing of trimers for E5(3,7) than E5(4,8) particularly at neutral pH can be rationalized by noting the enhanced repulsion between the interfacial glutamic side chains at positions 4 and 8, but not at 3 and 7.

As shown in Fig. 3B, FRET experiments between NBD (donor) and rhodamine (acceptor) moieties conjugated to the N-terminus to the two E5 and HA2(1–25) analogs provided more direct evidence for the self-assembly of the peptide molecules in the membranes. The energy transfer efficiency measured on the labeled analogs is much higher than that calculated with the assumption of random distribution of the molecules using 50 Å Förster distance for the NBD–rhodamine pair. It is noted that HA2(1–25) has a tighter packing than do the two E5 analogs, and E5(3,7) associates more tightly than E5(4,8) as revealed by this long range probe. The more compact intra-trimer interaction for E5(3,7) than E5(4,8) may arise from the stronger hydrogen bond formed between Glu3 carboxylic group and the N-terminal amino hydrogen within the trimer than the corresponding bond involving the Glu4 carboxylic group (see the Discussion).

3.4. Gel electrophoresis experiments revealed a strong tendency of the fusion peptide analogs to oligomerize in the lipidic environment

To further examine the propensity of self-assembly of the fusion peptides in the membrane, PFO-PAGE measurements were performed and the results are displayed in Fig. 4. Both E5 variants exhibit oligomeric species (with the oligomeric order of 6 to 7) under the shearing electric field at pH 4.8 and 7.4. Several observations can be made, including that the order of aggregation tends to be higher as pH is lowered and the major species of E5(3,7) have smaller molecular mass than that of E5(4,8). Together with Fig. 3, it is clear that the peptide analogs have propensity of forming oligomers in the membrane at acidic and neutral pH.

3.5. Polarity of the environment of the glutamic acid side chains of the E5 peptides in SDS micelles can be deduced from NMR data

Fig. 5 shows the variation with pH of ^1H chemical shift of the five glutamic acid residues on each of the two peptides. The $\Delta\delta$ (titration shift), pK_a and Hill coefficient extracted from the non-linear least square fit of Eq. (1) are

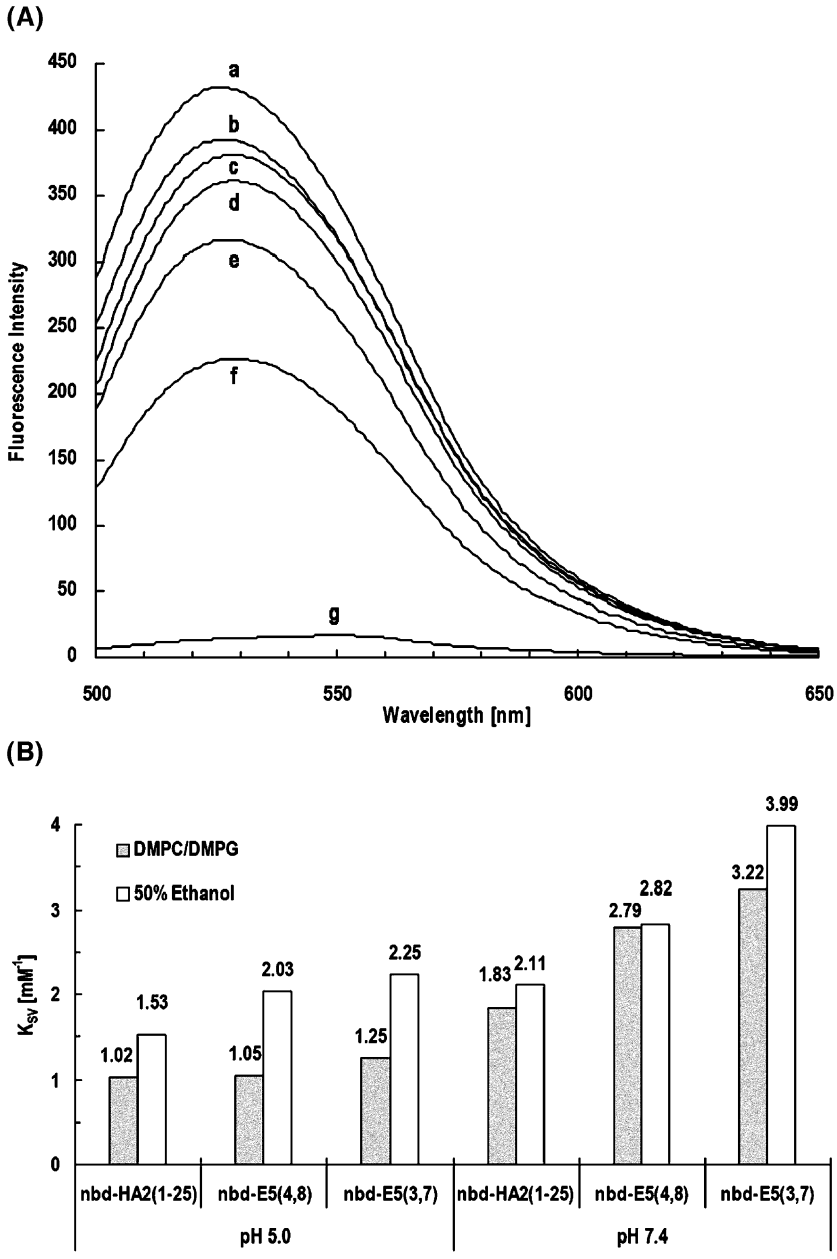

Fig. 2. (A) NBD fluorescence of the N-terminally labeled HA2(1–25), E5(4,8) and E5(3,7) at pH 5.0 and 7.4 in DMPC:DMPG vesicles. Traces: a and b, HA2(1–25) at pH 5.0 and 7.4, respectively; c and d, E5(4,8) at pH 5.0 and 7.4, respectively; e and f, E5(3,7) at pH 5.0 and 7.4, respectively. Trace g displays NBD fluorescence profile of the labeled HA2(1–25) in aqueous solution at pH 5.0; other labeled peptides exhibit similar intensity and emission maximum and, therefore, are not shown. Note the dramatic increase in intensity and the blue shift in emission maximum (from 540 to ~526 nm) for all three peptides upon associating with the membrane. Both phenomena are indicative of a localization of the N-terminus of the fusion peptide analogs in a hydrophobic environment. HA2(1–25) displays higher intensity than the two Glu-rich analogs at the same pH, suggesting deeper penetration for the parent fusion peptide. The consistent pattern of slightly reduced intensity on neutralization for these three peptides may reflect a shallower insertion of the peptide into the membrane at higher pH. (B) pH dependence of K_{SV} of NBD fluorescence quenching by Co^{2+} for HA2(1–25), E5(4,8) and E5(3,7) to determine the position in the DMPC:DMPG vesicles of the N-terminal region of the peptides. K_{SV} obtained in 50% ethanol solution for each of the peptide analogs is used as the reference value for the quenching of surface-residing NBD by Co^{2+}. Increased K_{SV} with elevating pH for all three peptides indicates a movement toward the membrane surface of the N-terminus of the peptides upon neutralization. The smaller K_{SV} for HA2(1–25) compared to E5 analogs under the same condition likely reflects a slightly higher tendency to form oligomers and/or deeper immersion in the membrane for the parent peptide.

listed in Table 1. Several conclusions can be gleaned from the table. First, all the pK_a values are larger than that of glutamic acid residue in the model peptide (pK_a=4.3) measured by Bundi and Wüthrich [30] in aqueous medium, suggesting an environment less polar than water. In particular, the pK_a of Glu3 and Glu7 is close to 6, ~2 log units larger than the standard value, indicating a hydrophobic environment for the two residues [31].

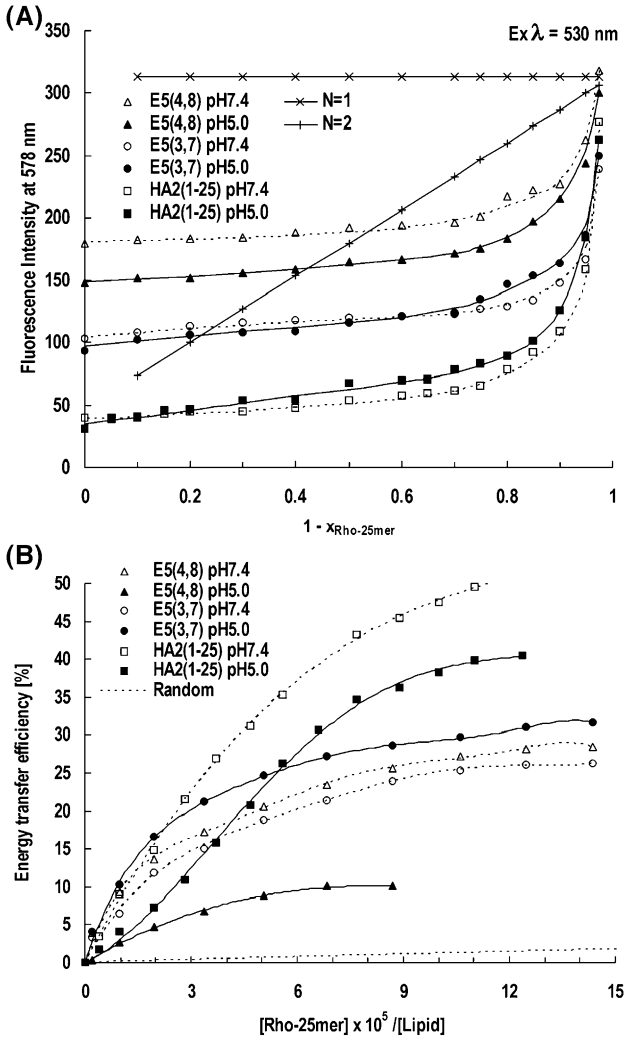

Fig. 3. (A) Variation of normalized fluorescence intensity with the composition of Rho-labeled E5 analogs and HA2(1–25) in DMPC:DMPG 1:1 vesicle, with the total concentration of the labeled and unlabeled peptide being held constant at 1 μM. The abscissa is the fraction of unlabeled fusion peptide. The profiles arising from $N=1$ and $N=2$ are shown to indicate that the molecular clustering of the peptides cannot be accounted for by a single mode of assembly; multi-mode clustering needs to be invoked and hence the existence of longer range interaction between the monomers. (B) Variation of NBD-to-rhodamine FRET efficiency with the ratio of rhodamine to the lipid (1:1 DMPC:DMPG). The NBD and rhodamine groups are labeled at the N-terminus of the fusion peptide analogs embedded in the vesicles. Considerably higher FRET efficiency for the three peptides than that obtained with random distribution of the peptides reflects self-association of the peptides in membranes. Higher FRET efficiency is found for the wild type peptide than the other Glu-rich analogs. The indicated order of packing-tightness, i.e., HA2(1–25)>E5(3,7)>E5(4,8) is exactly the same as that observed in Fig. 3A.

The scheme in Fig. 6 illustrates the pK_a change in relation to the free energy of transfer of Glu side chain from aqueous to less polar medium. It is noteworthy that the pK_a for Glu3 of E5(3,7) is higher than Glu4 of E5(4,8), suggesting that the side chain of Glu3 of E5(3,7) reside in a more hydrophobic environment than that of Glu4 of E5(4,8). Because the magnitude of pK_a shift for both Glu3 and Glu4 carboxyl groups is less than that observed by Smith et al. [8] for neu/erbB-2 receptor in the DMPC:DMPS membrane, we surmise that these two groups are embedded near the interfacial region and Glu4 is perhaps more hydrated than Glu3.

Moreover, the Hill coefficient of the carboxylic groups on Glu3 and Glu7 is each substantially smaller than 1. It is noteworthy that the deviation of both pK_a and Hill coefficient from the standard values for Glu4 and Glu8 in E5(4,8) is considerably smaller than Glu3 and Glu7 in E5(3,7). The pattern, in combination with the result that the N-terminal portion of the membrane-bound influenza fusion peptide immerses in the non-polar region of membrane, leads to the idea that positions 3 and 7 are more exposed to the hydrophobic interior of membrane than are positions 4 and 8 in the trimer. Consequently, the ionized form of the carboxyl group is more destabilized for residues 3 and 7 in E5(3,7) than are residues 4 and 8 in E5(4,8), resulting in a higher pK_a for the former analog; the interaction between the side chains of Glu3 and Glu7 is stronger than that between Glu4 and Glu8, leading to higher anti-cooperativity for the former analog. A similar finding was documented by Song et al. [14]; thus they observed a small Hill coefficient (~0.8) for the spatially proximate glutamic and aspartic acid residues of Turkey ovomucoid third domain variant. This result supports the notion that the side chains of Glu3 and Glu7 interact strongly with each other, probably due to their exposure to hydrophobic region of the micelle. As another line of evidence for Glu3 carboxyl moiety exposure to non-

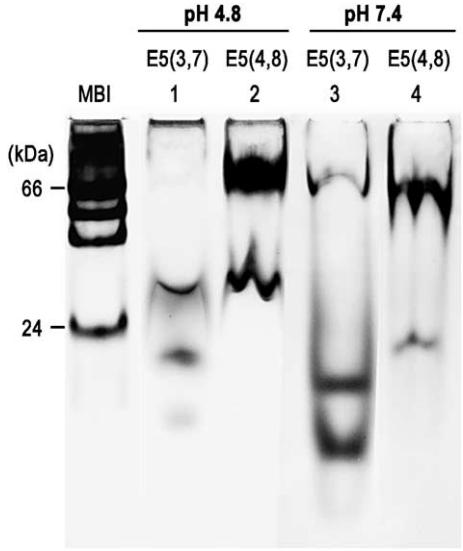

Fig. 4. PFO-PAGE data of E5(3,7) and E5(4,8) at pH 4.8 and 7.4. Peptides/lysoPC mixtures (0.5:3 mM) were resuspended in pH 4.8 buffer with 2% PFO or in pH 7.4 buffer with 1% PFO. The 18.3% polyacrylamide gel was prepared with pH 7.4 buffer containing 0.1% PFO. MBI represents a prestained protein ladder diluted (1:10) with the Laemmli loading buffer. Molecular weight markers (MW) have been determined by MALDI-TOF mass spectrometry. The two peptide analogs form predominantly oligomeric species of the order of 3 to 12, providing direct evidence of self-assembly for the charged peptides in the membranous environment.

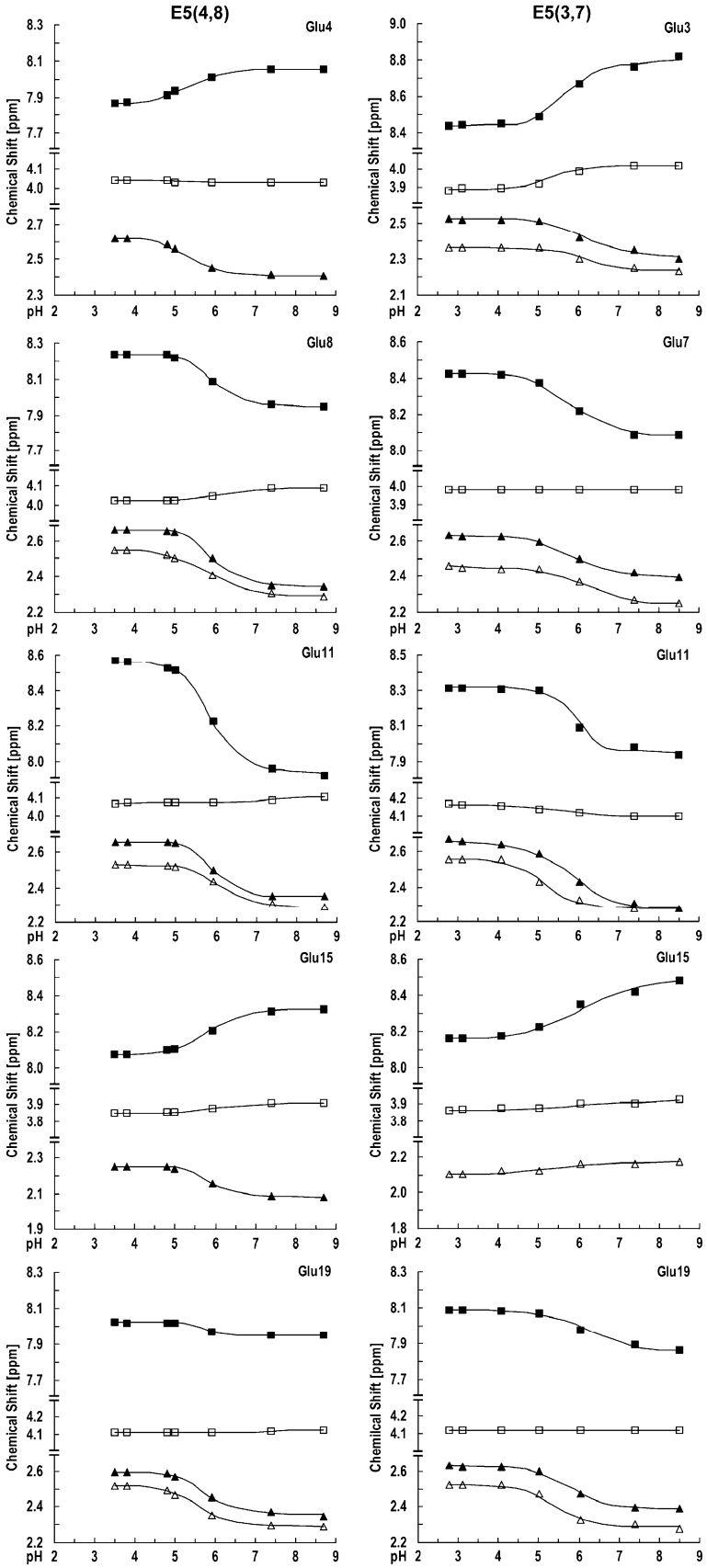

Fig. 5. ^{1}H chemical shift titration on E5(3,7) and E5(4,8) in SDS micellar solution. The data are used for the determination of the pK_a of several backbone and side chain ^{1}H under the influence of titratable groups, including induction effect via chemical bonds and through-space hydrogen bond, in the molecules. Different pK_a values can be distinguished between residues 3 and 7 in E5(3,7) and residues 4 and 8 in E5(4,8).

Table 1
^{1}H NMR chemical shifts, pK_a values and Hill coefficients of titratable residues and Asn12 of HA2(1–25), E5(4,8) and E5(3,7)[a]

Peptide	Residue	NMR signal	δ_A^- [ppm]	$\Delta\delta$ [ppm][b]	pK_a^c	Hill coefficient	Variation from model pK_a values[d]
HA2(1–25)	E11	NH	7.95	−0.54	5.81 (0.00)	1.24 (0.01)	1.51
		αH	4.10	0.01	N.D.	N.D.	N.D.
		β1	2.12	−0.05	N.D.	N.D.	N.D.
		β2	2.05	−0.09	N.D.	N.D.	N.D.
		γ2	2.32	−0.31	5.91 (0.00)	1.27 (0.01)	1.61
		γ3	2.26	−0.27	5.90 (0.00)	1.29 (0.01)	1.60
	N12	NH	8.10	0.07	5.79 (0.02)	2.59 (0.16)	
		αH	4.78	0.09	5.99 (0.01)	1.01 (0.03)	
		β	2.81	0.02	N.D.	N.D.	
		γNH1	7.60	0.01	N.D.	N.D.	
		γNH2	6.91	0.06	N.D.	N.D.	
	E15	NH	8.33	0.23	5.82 (0.01)	1.99 (0.04)	1.52
		αH	3.97	0.08	5.83 (0.01)	1.22 (0.03)	1.53
		β1	1.94	−0.03	N.D.	N.D.	N.D.
		β2	1.91	0.04	N.D.	N.D.	N.D.
		γ2	2.13	−0.17	5.33 (0.00)	0.88 (0.01)	1.03
		γ3	2.09	−0.12	5.16 (0.01)	0.83 (0.01)	0.86
	D19	NH	7.99	−0.16	5.43 (0.01)	1.01 (0.02)	1.53
		αH	4.55	−0.01	N.D.	N.D.	N.D.
		β	2.69	−0.20	5.19 (0.00)	1.17 (0.01)	1.29
E5(4,8)	E4	NH	8.06	0.19	5.30 (0.09)	0.89 (0.15)	1.00
		αH	4.03	−0.01	N.D.	N.D.	N.D.
		β1	2.19	−0.04	N.D.	N.D.	N.D.
		β2	2.07	−0.08	5.40 (0.05)	1.13 (0.11)	1.10
		γ[e]	2.41	−0.21	5.37 (0.02)	1.10 (0.05)	1.07
	E8	NH	7.95	−0.29	5.86 (0.04)	1.35 (0.25)	1.56
		αH	4.09	0.07	6.07 (0.12)	1.33 (0.76)	1.77
		β1	2.12	−0.12	5.53 (0.03)	1.37 (0.08)	1.23
		β2	2.05	−0.10	5.65 (0.04)	1.83 (0.22)	1.35
		γ2	2.35	−0.31	5.92 (0.01)	1.35 (0.09)	1.62
		γ3	2.29	−0.26	5.83 (0.02)	0.77 (0.03)	1.53
	E11	NH	7.93	−0.64	5.86 (0.02)	1.07 (0.07)	1.56
		αH	4.11	0.04	7.46 (0.54)	0.73 (0.65)	3.16
		β[e]	2.06	−0.10	5.70 (0.04)	1.98 (0.32)	1.40
		γ2	2.35	−0.31	5.90 (0.01)	1.61 (0.14)	1.60
		γ3	2.29	−0.24	6.08 (0.02)	1.06 (0.07)	1.78
	N12	NH	8.10	0.03	N.D.	N.D.	
		αH	4.77	0.11	5.85 (0.01)	0.67 (0.01)	
		β	2.82	0.04	N.D.	N.D.	
		γNH1	7.71	0.15	5.70 (0.01)	0.77 (0.02)	
		γNH2	6.99	0.13	5.38 (0.01)	0.92 (0.02)	
	E15	NH	8.32	0.25	5.84 (0.07)	0.90 (0.14)	1.54
		αH	3.90	0.05	5.93 (0.15)	1.02 (0.41)	1.63
		β1	1.88	−0.04	5.34 (0.02)	0.61 (0.02)	1.04
		β2	N.D.		N.D.	N.D.	N.D.
		γ2	2.08	−0.17	5.81 (0.02)	1.37 (0.11)	1.51
		γ3	N.D.		N.D.	N.D.	N.D.
	E19	NH	7.95	−0.08	5.62 (0.19)	1.45 (0.63)	1.32
		αH	4.12	0.01	N.D.	N.D.	N.D.
		β[e]	2.06	−0.03	N.D.	N.D.	N.D.
		γ2	2.35	−0.25	5.77 (0.02)	1.08 (0.05)	1.47
		γ3	2.29	−0.23	5.51 (0.02)	1.10 (0.04)	1.21
E5(3,7)	E3	NH	8.82	0.38	5.80 (0.01)	0.94 (0.01)	1.50
		αH	4.02	0.14	5.51 (0.01)	0.96 (0.01)	1.21
		β[e]	2.03	−0.09	6.24 (0.02)	0.40 (0.01)	1.94
		γ2	2.30	−0.23	6.33 (0.00)	0.60 (0.00)	2.03
		γ3	2.23	−0.13	6.06 (0.00)	1.18 (0.02)	1.76

(continued on next page)

Table 1 (*continued*)

Peptide	Residue	NMR signal	δ_A^- [ppm]	$\Delta\delta$ [ppm][b]	pK_a^c	Hill coefficient	Variation from model pK_a values[d]
E5(3,7)	E7	NH	8.09	−0.34	5.84 (0.01)	0.96 (0.01)	1.54
αH		3.98	0.00	N.D.	N.D.	N.D.	
β1		2.11	−0.07	6.17 (0.01)	0.96 (0.02)	1.87	
β2		2.00	0.00	N.D.	N.D.	N.D.	
γ2		2.40	−0.23	5.91 (0.00)	0.74 (0.00)	1.61	
γ3		2.25	−0.21	6.26 (0.00)	0.83 (0.01)	1.96	
	E11	NH	7.94	−0.37	5.89 (0.00)	1.51 (0.03)	1.59
		αH	4.10	−0.07	N.D.	N.D.	N.D.
		β1	2.07	−0.09	5.36 (0.01)	0.85 (0.01)	1.06
		β2	2.01	−0.04	5.98 (0.01)	1.12 (0.04)	1.68
		γ2	2.28	−0.39	5.79 (0.00)	0.73 (0.00)	1.49
		γ3	2.28	−0.28	5.13 (0.00)	0.88 (0.00)	0.83
	N12	NH	8.29	0.25	5.10 (0.02)	0.75 (0.02)	
		αH	4.90	0.16	5.27 (0.02)	2.24 (0.20)	
		β	2.74	−0.04	N.D.	N.D.	
		γNH1	7.54	0.04	N.D.	N.D.	
		γNH2	6.93	0.05	N.D.	N.D.	
	E15	NH	8.48	0.32	5.82 (0.01)	0.60 (0.01)	1.52
		αH	3.92	0.06	6.43 (0.12)	0.25 (0.02)	2.13
		β1	N.D.		N.D.	N.D.	N.D.
		β2	1.96	0.12	4.99 (0.02)	0.25 (0.01)	0.69
		γ2	N.D.		N.D.	N.D.	N.D.
		γ3	2.17	0.07	N.D.	N.D.	N.D.
	E19	NH	7.86	−0.23	6.08 (0.01)	0.79 (0.01)	1.78
		αH	4.12	0.00	N.D.	N.D.	N.D.
		β[e]	2.06	−0.05	N.D.	N.D.	N.D.
		γ2	2.39	−0.24	5.77 (0.00)	1.15 (0.01)	1.47
		γ3	2.28	−0.24	5.48 (0.00)	1.19 (0.00)	1.18

[a] The numbers in parentheses are the standard deviations returned by the software package fitting the titration curves.
[b] $\Delta\delta = \delta_A^- - \delta_{HA}$.
[c] N.D. denotes that pK_a and Hill coefficient values cannot be precisely determined mainly due to small titration shift (< 0.1 ppm, in general).
[d] The standard pK_a values assumed here were 3.9±0.1 for Asp and 4.3±0.1 for Glu, which were reported by Bundi and Wüthrich [33].
[e] The degeneracy of the resonances of Glu4 CγH, Glu11 CβH and Glu19 CβH of E5(4,8) and of Glu3 CβH and Glu19 CβH of E5(3,7).

polar environment, the larger magnitude of a positive $\Delta\delta$ for Glu3 NH than for Glu4 NH is a manifestation of stronger hydrogen bond of the Glu3 NH to side chain carboxyl group as a result of more exposure of the latter group to the hydrophobic medium.

Some common features can be observed from Glu11, Glu15 and Glu19 for the two peptide analogs in Fig. 5 and

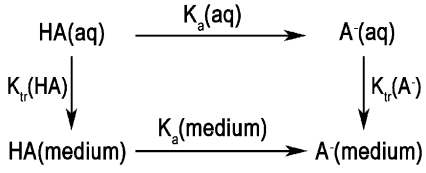

Fig. 6. Schematic diagram of ionization of a carboxyl group on the side chain of glutamic or aspartic acid in different media to illustrate a shift of pK_a to a higher value in a hydrophobic environment. Since the processes involved in the scheme are in a thermodynamics cycle, the sum of the free energy of the four reactions $\Delta G_{total}=0$. Because $\Delta G=-RT\ln(K)$, $K_{tr}(HA)/K_{tr}(A^-)=K_a(aq)/K_a(medium)$. Here, the medium represents a membranous environment, which could be the acyl chain domain of the membrane or interfacial region; K_{tr} denotes the partition coefficient of the protonated or ionized state. Because the free energy of transfer from aqueous phase to membranous medium for the polar HA is less positive than that for the ionic A^-, $K_{tr}(HA)/K_{tr}(A^-)$ is greater than unity. Hence, pK_a(medium) is larger than pK_a(aq).

summarized in Table 1. For example, the Glu15 side chain exhibits moderate anti-cooperativity, implying hydrogen bond formation with other acceptor group(s), possibly with Glu11 (especially for E5(3,7), which has slightly lower pK_a and enhanced anti-cooperativity for Glu11). Glu19 displays no cooperativity or anti-cooperativity, indicating no strong hydrogen bond interaction with other side chains, perhaps because it is most C-terminal among the five acidic residues and has less helical character. The more isolated nature of Glu19 in both E5 analogs is manifested in the significantly smaller $\Delta\delta$ for the backbone NH (Table 1). A substantially larger $\Delta\delta$ for the amide proton of Glu11 than other Glu residues in the same molecule in all three analogs suggests a conformational change near Glu11 with pH. The idea is supported by a substantial larger $\Delta\delta$ for CαH of Asn12 (~0.1 ppm) and Glu15 (~0.06 ppm) than the CαH of other Glu residues since the chemical shift of CαH is less susceptible to the effect of hydrogen bond and through bond induction from the carboxyl group. In this context, it is of interest that an HA2 analog exhibited pH-dependent structural alteration near Asn12 in the micelle-bound state [32]. Additionally, a downfield shift of the backbone amide proton resonance at higher pH for Glu3 and Glu4 suggests that it forms an intraresidue hydrogen bond with the

carboxyl group, likely due to the absence of carbonyl group in the N-terminal direction to form hydrogen bonds to the amide protons at these positions in a helix and its exposure to the apolar environment as is elaborated in the Discussion section; again, larger $\Delta\delta$ for Glu3 NH indicates that the hydrogen bond is stronger than that formed with Glu4 NH, consistent with the idea that Glu3 resides in a more hydrophobic environment leading to stronger hydrogen bond.

As another corroborative result, the two CγH in Glu3 of E5(3,7) are non-equivalent but degenerate in Glu4 in E5(4,8), suggesting that the former is involved in stronger hydrogen bond than the latter. The result is in line with the concept that Glu3 of E5(3,7) is exposed in more hydrophobic environment than Glu4 of E5(4,8).

$\Delta\delta$ values for the backbone NH vary from 0.08 to 0.63 ppm for the acidic residues under examination. From the direction of NH chemical shift dependence on pH and the magnitude, it is clear that Glu11 of E5(4,8)–and, to a less extent, of E5(3,7)–undergoes substantial conformational change with pH titration. This conclusion is consistent with the near unity of Hill coefficient for the two Glu11 NHs, indicating little cooperativity in the pH profile of the chemical shift of these protons, which would be expected to display anti-cooperativity as a hydrogen bond donor. The downfield shift with increasing pH of NHs of both Glu residues near the N-terminus (namely Glu3 and Glu4 for E5(3,7) and E5(4,8), respectively) suggests that the amide proton is hydrogen bonded to the carboxyl group on the side chain of the residue [33]. This interpretation is supported by the same pH dependence of the chemical shift of NHs of Leu2 and Phe3 for the two E5 peptide variants. Conceivably, the formation of hydrogen bond would dampen the negative charge on the Glu side chain at high pH; the gain in free energy is especially large for the carboxyl group embedded in a highly hydrophobic environment. It is therefore likely that the carboxyl groups of these two Glu residues form hydrogen bonds with the free amino groups at the N-terminus, as hinted by the Gly1 CαH titration shift of E5(3,7) with a pK_a value of ~5.5 and a $\Delta\delta$ of ~−0.1 ppm (arising from shielding of the negative charge of Glu3 carboxyl group). The fact that the positive $\Delta\delta$ value is larger for the NH of Glu3 in E5(3,7) than that of Glu4 in E5(4,8) (0.38 vs. 0.19 ppm) may reflect the capacity of forming a stronger hydrogen bond for the former carboxyl group as a result of its higher degree of exposure to the apolar milieu of the micelle. The Hill coefficient of the chemical shift for CγH of Glu3 and Glu7 is significantly <1 (0.6 and 0.74, respectively), consistent with the idea of electrostatic interaction between these two side chains, which is likely a result of enhanced interaction between the polar groups in the hydrophobic environment. In contrast, the Hill coefficient for CγH of Glu4 and Glu8 is closer to unity (1.1 and 1.3, respectively), indicating little anti-cooperativity, consistent with little interaction between the two side chains of Glu4 and Glu8 residues in more polar environment (see Discussion below).

4. Discussion

4.1. Self-assembly of HA2(1–25) and the two E5 analogs in the membrane-mimic environment is detected by rhodamine fluorescence self-quenching and PFO-PAGE experiments

Fig. 2A and B show that the N-terminal portion of the three HA2 fusion peptide analogs penetrated into the hydrophobic core of membrane bilayer at pH 5.0 while resides closer to the membrane interface at pH 7.4 (yet in a hydrophobic environment according to NBD data of Fig. 2B), presumably caused by the ionization of the acidic groups. The altered topography of the N-terminus of the peptide analogs with pH may lead to diminished perturbation on the membrane for the fusion peptide at neutral pH, accounting, in part, for the pH sensitivity of the lipid mixing activity of the peptides [17]. Because it is highly energetically unfavorable for peptides with charged or polar residues to be embedded in the apolar medium as monomers, we surmised that the two peptides self-assembled in the membrane. This is vindicated in Fig. 3A, which, however, does not determine the exact order of oligomerization but exhibits multi-modal self-association. Interestingly, a double peak (7.3 and 10.8 Å) distribution has been observed in the distribution of interhelix distance of bundled and polytopic helical membrane proteins [34].

Further support of self-association comes from results on the energy transfer between NBD and rhodamine displayed in Fig. 3B, which monitors longer range (~50 Å) interaction. Note that tighter association is observed for pH 7.4 than pH 5.0 for HA2(1–25) and E5(4,8). This suggests that the closer packing of the fusion peptide does not correlate with fusion activity; instead, we postulate that a loose, but not rigid, intermolecular association which is capable of altering the state of packing or clustering during various stages of fusion reaction (e.g. in the initial membrane insertion and in the recruitment of the fusion proteins to form fusion pores) is essential for the fusion activity of the fusion peptide. Remarkably, both Fig. 3A and B indicate that HA2(1–25) has the highest degree of association among the three analogs, in support of the assertion that the glycine residue enhances interactions between the proteins in the membrane [26].

In Fig. 4, the order of self-association was observed between 3 to 12 in the PFO-PAGE measurements for the two Glu-rich analogs with lower pH, yielding higher order oligomer and E5(4,8) forming higher species than E5(3,7) under the same pH. The same trends have been observed in the SDS-PAGE experiments on these fusion peptide analogs (cf. Supplementary data). The consistent observation of slightly higher mass species formed by E5(4,8) than E5(3,7) suggests a moderate effect of charged residues at positions 4

and 8 in promoting inter-monomer association than at positions 3 and 7 for the Glu-rich peptide analogs. The variation in insertion depth and self-association with pH for these membrane-active peptides may have bearing on their pH-sensitive activity. The findings are somewhat at odd with the conclusion drawn by Han and Tamm [35] on the pH dependence of the self-association of the influenza fusion peptide analog in the membrane—the peptides exist as monomeric helix at pH 5.0 but predominantly transform into β-sheet aggregate at pH 7. Since trimeric assembly has been found for the ectodomain of hemagglutinin [36] and HA2, we used accordingly a trimeric model for the fusion peptide analogs in Fig. 1 for further characterization. The model revealed that positions 3, 4, 7 and 8 are critical in forming oligomers at neutral and mild acidic pH in the model membrane.

4.2. NMR data indicate that (1) hydrogen bonds form between the carboxyl and the N-terminal free amine groups and between the carboxyl and amide groups in the N-terminal of the E5 fusion peptide analogs; (2) the Glu11–Glu15 region undergoes structural change with pH change from 5.0 to 7.4

Having established the location in the hydrophobic region of the membrane and the oligomerization propensity for the peptide analogs, we used NMR data to further investigate the factors that determine the interaction between the peptide molecules in the membranous setting as opposed to the aqueous medium. Of particular interest is the charge–charge interaction in the hydrophobic membrane interior, because the Glu residues are located in or close to the highly apolar milieu.

The pK_a of the Glu carboxyl groups in both E5 variants in SDS micelle monitored by the side chain and backbone ^{1}H chemical shift titration is sensitive to, and hence provides information regarding, the environment of various Glu residues in the detergent micelle [37]. All pK_a values exhibit one to two units higher than the pK_a of water-solvated Glu side chain, implying that these residues are embedded in the apolar environment since intraresidue hydrogen bond of amide proton to the Glu side chain carboxyl group would result in a lower pK_a (Fig. 6). Together with pK_a values for the Glu residues in HA2(1–25) showing also elevated pK_a (Table 1), the results provide direct evidence that data at pH 5.0 and 7.4 correspond to protonation and deprotonation states, respectively, for the influenza fusion peptide analogs in model membranes. Similarly, a pK_a of 7.5 for the Glu carboxyl group [38] has been observed and was attributed to its location in a hydrophobic cavity in a protein. The observed pK_a values of close to 6 for the side chains on Glu3 and Glu7 of E5(3,7) and on Glu4 and Glu8 of E5(4,8) are consistent with the interpretation, since these residues reside in the micellar hydrocarbon core. Higher pK_a values for small organic acids such as propionic acid in solvents less polar than water have been documented [31].

According to Fig. 3A, both E5 analogs are self-associated in a non-single mode in the membranes. We hypothesize that the peptide molecules in the membrane pack more tightly as trimer, which is surrounded by other trimers separated by longer distances. The inspection of the trimeric model for the association of peptide helices in Fig. 1 shows that Glu3 and Glu7 in E5(3,7) are more exposed to the hydrophobic membrane hydrocarbon core than are Glu4 and Glu8 in E5(4,8). The higher pK_a of the side chain (6.2 for Glu3 vs. 5.4 for Glu4) and the larger positive titration shift for the amide proton of Glu3 than the corresponding values of Glu4 provides evidence for the model. Thus, to reduce the free energy cost of the polar side chain exposure, stronger hydrogen bonds are formed between the Glu3 carboxyl group and the amide proton and between the carboxyl group and N-terminal amine protons, as seen by the positive $\Delta\delta$ value for the amide proton chemical shift of Glu3 (and the amide proton of Leu2, S.F. Cheng. and D.K. Chang, unpublished data). The concept is corroborated by the striking titration shift of ~0.1 ppm for Gly1 CαH of E5(3,7) with a pK_a of 5.5, as opposed to near constancy for the counterpart in E5(4,8) or HA2(1–25). Furthermore, a strong electrostatic interaction between the polar groups of Glu3 and Glu7 side chains is indicated by a higher anti-cooperativity in the chemical shift titration observed with Glu3 and Glu7 side chain protons compared with that of Glu4 and Glu8 (Table 1). Conversely, given that the side chains of Glu4 and Glu8 are on the polar face of the trimer, the energetic gain of forming hydrogen bond is not as large, as manifested in the smaller positive $\Delta\delta$ of Glu4 amide proton than that of Glu3. Of note is the degeneracy of CγH of Glu4 yet two distinct resonance peaks can be identified for the two CγH of Glu3 (Fig. 4) under all pH tested; the observation supports the idea that the Glu3 side chain is involved in stronger hydrogen bond(s) yielding splitting of CγH signals due to hindered rotational freedom around the Cβ–Cγ bond but not for Glu4. It can therefore be concluded that the exposure of the polar groups to more apolar milieu and the closeness to the N-terminal region for Glu3 and Glu7 result in strong interaction of these two side chains and hydrogen bond formation between Glu3 side chain and amide/amine protons on the N-terminal residues. The difference in the order of oligomerization seen in PFO-PAGE measurements between the two Glu-rich analogs (Fig. 4) may be attributed in part to the exposure to the hydrophobic medium of the Glu3 and Glu7 side chains in the context of the model in Fig. 1. It should be noted that, in addition to the ionic interaction between the groups within the same monomer, the possibility that the interaction between the groups from neighboring monomers cannot be excluded.

It is of interest to note that the charge–charge interaction between basic residues of T cell receptor α or β and acidic residues of CD3 δ or ϵ in the TM domain was found critical for the organization of the TCR-CD3 complex and therefore the cellular signal transduction [19]; the model is similar to our result in that the interaction between Glu3 or 4 side

chain and N-terminal amino group is an integral component of the assembly of E5 fusion peptide analogs in the model membrane.

A single replacement of Val by Glu at position 664 in the hydrophobic membrane-spanning domain of neu/erbB-2 receptor is thought to stabilize receptor dimers and cause constitutive activation and cell transformation in the absence of ligand [8]. Of note is that the Glu substitution at position 663 or 665 does not have a detectable effect [29]. From NMR study, the pK_a of the Glu mutant was determined to be around 6.5 and 8.5 in DMPC and in DMPC:DMPS vesicles, respectively. Strong hydrogen bonding was also found for the Glu variant and was attributed to stabilize dimers in the membrane. The pK_a is somewhat higher than what we measured for the Glu3 carboxyl of E5(3,7) in SDS micelles. It is probable that the environment is more polar for the Glu3 carboxyl of E5(3,7) with a nearby Glu7 in the micelle than for Glu664 carboxyl of the neu/erbB-2 receptor in the vesicles; consequently, the hydrogen bond participated by the Glu3 carboxyl, which may stabilize a loose trimer–trimer association, is not as strong and hence a smaller pK_a shift.

The conformational change in the Glu11–Glu15 stretch of the three fusion peptides tested on pH alteration from 7.4 to 5.0 can be deduced from a large and positive shift titration of Glu15 and Asn12, in agreement with the Han et al. [32] report on an HA2 fusion peptide analog.

The direction and magnitude of chemical shift variation with pH for the Glu15 amide protons of all three peptide analogs investigated suggest that these protons form intra-residue hydrogen bond to the carboxyl groups and the region around Glu15 likely undergoes conformational change with pH. The latter possibility is in line with the NMR and EPR studies of a HA2 fusion peptide analog by Han et al., in which a kink in the helical structure was found near Asn12 at pH 5 and the region C-terminal to Asn12 becomes more unordered at pH 7.4 [32].

Charged residues are occasionally found in the apolar interior of membrane in membrane-spanning proteins mostly for proton and electron transport and binding to prosthetic groups. For gp41, the transmembrane fusion protein of HIV-1, an arginine is located near the center of the putative transmembrane domain. Since gp41 is thought to trimerize on the viral surface, the presence of arginine probably contributes to the oligomerization of the fusion protein to reduce the energetic penalty of exposing the charge in the membrane core. The role of ionizable residues of the transmembrane helices in the membrane interior has been shown to modulate the oligomerization and insertion depth [39]. The four negatively charged residues have been implicated in the trafficking of a protein kinase from Golgi apparatus to the plasma membrane via a conformational change, exposing the charged residues [40]. A Val-to-Asp mutation in the cystic fibrosis transmembrane conductance regulator has been demonstrated to enhance the helix–helix association in the membrane via proposed interhelical hydrogen bonds and leads to a disease state [41]. Both reports underscore a critical role of charged residues in the protein processing and function through alteration in structure and organization.

Hydrophilic residues such as Asn have been determined to stabilize the oligomerization of hydrophobic peptides in micelles [42,43]. In the present work, self-assembly has been shown to exist for the two highly negatively charged peptides at neutral and acidic pH. The position and ionization state of Asp was found to cause a dramatic alteration in the topology of the inserted peptides by Caputo and London [44]. In comparison, we have observed a moderate change in insertion depth and a slight change in oligomerization with pH variation between 5.0 and 7.4 that changes the ionization state of Glu residues in the peptides.

Our data on the NBD-quenching with cobalt ion (Fig. 2B) indicate that the effect of ionization arising from pH change has a significant effect on the distance of the N-terminally labeled NBD from the membrane surface. Similarly, a previous investigation by Monné et al. [45] concluded that the negatively charged residues Asp and Glu caused a change in the location of the transmembrane helix when these residues are placed in the one to two C-terminal turns but not when placed more centrally. Our result thus concurs with this study but it is noted in our interpretation that the carboxyl groups on Glu3 and Glu4 form hydrogen bond or ionic interactions between their side chains and the free N-terminal amino groups at pH 5.0 and 7.4.

We have observed a decreased propensity for self-aggregation (Fig. 3A and B) and shallower immersion (Fig. 2B) in the membrane for the E5 analogs on neutralization; both phenotypes could contribute to the pH dependence of the lipid activity of the Glu-rich fusion peptides [17].

The analysis of helical structures of transmembrane and soluble proteins by Eilers et al. [34] revealed that, in the membrane, glycine has the highest score in the tendency to be packed in the interhelical region; unexpectedly, moderately high scores were found for Asn, Gln, Asp and Glu residues, probably also due to hydrogen bonds, as described for serine and threonine—at least at acidic pH for the two negative charged residues. The oligomerization of the two E5 variants provides direct evidence for the packing of negatively charge-containing peptides in the membrane or membrane-mimic medium.

The low dielectric medium of the apolar membrane core enhances the interaction energy of ion pairing and hydrogen bond [46]; hence, the interaction between the carboxyl groups of the E5 variants is probably mediated by hydrogen bond at pH 5.0 and by ionic force at neutral pH with protons (or other counterions) acting as the counterions, thus damping the effect of hydrophobicity of lipid hydrocarbon chains. In addition, water molecules may be present in the intermonomer space, creating a more polar local environment [47]. The latter effect may account in part for the lower pK_a of Glu4 NH of E5(4,8) than that of Glu3 NH of E5(3,7) since positions 4 and 8 are assumed on the face away from

the lipid core region as illustrated in Fig. 1. It is noted that the hydrogen bond and ionic force discussed here may be of both intra- and inter-monomeric in nature. The more polar central domain surrounded by apolar milieu of lipid acyl chains generated by self-association apparently stabilizes the oligomers, as manifested in Fig. 3. Better shielding from the hydrophobic environment of the carboxyl groups on positions 4 and 8 compared to those on positions 3 and 7–as evidenced by the lower pK_a of Glu4 and Glu8 in E5(4,8) than that of Glu3 and Glu7 in E5(3,7)–may account in part for the slightly higher order of oligomerization of E5(4,8) observed in PFO-PAGE measurements (Fig. 4). More explicitly, the stronger intramolecular (and intra-trimeric) hydrogen bond between Glu3 side chain and N-terminal amino group elevates pK_a of the Glu3 carboxyl group and renders weaker the inter-trimeric association for E5(3,7) compared to E5(4,8). This shielding-from-hydrophobic surrounding argument can also account for the shallower penetration of E5(3,7) than E5(4,8) (Fig. 2B). Interestingly, an increased hydration in membrane bilayer has been deduced from a smaller blue shift of Trp fluorescence of a labeled-*E. coli* LamB signal peptide containing polar residues Ser and Gln inserted into the membrane [48]. Water molecules have been found to be an integral component of protein folding and structures and a mediator of protein functions by forming hydrogen and ionic bonds with charged residues [49,50].

In the present work, we have studied the topology of charge-containing peptides and proposed that the charged residues in the membrane apolar core can be stabilized by ionic force, hydrogen bonds and the interstitial water molecules between polar residues in the interior of the membrane helix bundle. The concept may be useful in elucidating the mechanism of ion and biomolecular transporters, such as ligand gated ion channels [51] and glucose transporters [52], with regard to the conformational change and energetic profile.

Acknowledgements

Financial supports from Academia Sinica and National Science Council (NSC 92-2113-M-001-046), Republic of China, are gratefully acknowledged.

Appendix A. Supplementary data

Supplementary data associated with this article can be found, in the online version, at doi:10.1016/j.bbamem.2005.04.003.

References

[1] I. Markovic, E. Leikina, M. Zhukovsky, J. Zimmerberg, L.V. Chernomordik, Synchronized activation and refolding of influenza hemagglutinin in multimeric fusion machines, J. Cell Biol. 155 (2001) 833–843.
[2] A. Mittal, J. Bentz, Comprehensive kinetic analysis of influenza hemagglutinin-mediated membrane fusion: role of sialate binding, Biophys. J. 81 (2001) 1521–1535.
[3] H. Ellens, J. Bentz, D. Mason, F. Zhang, J.M. White, Fusion of influenza hemagglutinin-expressing fibroblasts with glycophorin-bearing liposomes: role of hemagglutinin surface density, Biochemistry 29 (1990) 9697–9707.
[4] R. Blumenthal, D.P. Sarkar, S. Durell, D.E. Howard, S.J. Morris, Dilation of the influenza hemagglutinin fusion pore revealed by the kinetics of individual fusion events, J. Cell Biol. 135 (1996) 63–71.
[5] T. Danieli, S.L. Pelletier, Y.I. Henis, J.M. White, Membrane fusion mediated by the influenza virus hemagglutinin requires the concerted action of at least three hemagglutinin trimers, J. Cell Biol. 133 (1996) 559–569.
[6] S.F. Cheng, A.B. Kantchev, D.K. Chang, Fluorescence evidence for a loose self-assembly of the fusion peptide of influenza virus HA2 in the lipid bilayer, Mol. Membr. Biol. 20 (2003) 345–351.
[7] Y. Kimura, K. Kurzydlowski, M. Tada, D.H. McLennan, Phospholamban inhibitory function is activated by depolymerization, J. Biol. Chem. 272 (1997) 15061–15064.
[8] S.O. Smith, C.S. Smith, B.J. Bormann, Strong hydrogen bonding interactions involving a buried glutamic acid in the transmembrane sequence of the neu/erbB-2 receptor, Nat. Struct. Biol. 3 (1996) 252–258.
[9] J.D. Lear, W.F. De Grado, Membrane binding and conformational properties of peptides representing the NH2 terminus of influenza HA2, J. Biol. Chem. 262 (1987) 6500–6505.
[10] D.K. Chang, S.F. Cheng, V.D. Trivedi, S.H. Yang, The amino-terminal region of the fusion peptide of Influenza virus hemagluttinin HA2 inserts into sodium dodecyl sulfate micelle with residues 16–18 at the aqueous boundary at acidic pH, J. Biol. Chem. 275 (2000) 19150–19158.
[11] M. Murata, S. Takahashi, S. Kagiwada, A. Suzuki, S. Ohnishi, pH-Dependent membrane fusion and vesiculation of phospholipid large unilamellar vesicles induced by amphiphilic anionic and cationic peptides, Biochemistry 31 (1992) 1986–1992.
[12] P.V. Dubovskii, H. Li, S. Takahashi, A.S. Arseniev, K. Akasaka, Structure of an analog of fusion peptide from hemagglutinin, Protein Sci. 9 (2000) 786–798.
[13] C.H. Hsu, S.H. Wu, D.K. Chang, C.P. Chen, Structural characterizations of fusion peptide analogs of influenza virus hemagglutinin, J. Biol. Chem. 277 (2002) 22725–22733.
[14] J. Song, M. Laskowski Jr., M.A. Qasim, J.L. Markley, NMR determination of pKa values for Asp, Glu, His, Lys mutants at each variable contiguous enzyme-inhibitor contact position of the turkey ovomucoid third domain, Biochemistry 42 (2003) 2847–2856.
[15] T. Szyperski, W. Antuch, M. Schick, A. Betz, S.R. Stone, K. Wüthrich, Transient hydrogen bonds identified on the surfaced of the NMR solution structure of Hirudin, Biochemistry 33 (1994) 9303–9310.
[16] P. Cosson, S.P. Lankford, J.S. Bonifacino, R.D. Klausner, Membrane protein association by potential intramembrane charge pairs, Nature 351 (1991) 414–416.
[17] E.A.B. Kantchev, S.F. Cheng, C.W. Wu, H.J. Huang, D.K. Chang, Secondary structure, phospholipid membrane interactions, and fusion activity of two glutamate-rich analogs of influenza hemagglutinin fusion peptide, Arch. Biochem. Biophys. 425 (2004) 173–183.
[18] D.M. Cortes, L.G. Cuello, E. Perozo, Molecular architecture of full-length KcsA. Role of cytoplasmic domain in ion permeation and activation gating, J. Gen. Physiol. 117 (2001) 165–180.
[19] M.E. Call, J. Pyrdol, M. Wiedmann, K.W. Wucherpfennig, The organizing principle in the formation of the T cell receptor–CD3 complex, Cell 111 (2002) 967–979.
[20] I.M. Williamson, S.J. Alvis, A.M. East, A.G. Lee, The potassium

channel KcsA and its interaction with the lipid bilayer, Cell. Mol. Life Sci. 60 (2003) 1581–1590.
[21] D. Rapaport, Y. Shai, Interaction of fluorescently labeled pardaxin and its analogues with lipid bilayers, J. Biol. Chem. 266 (1991) 23769–23775.
[22] B.K.-K. Fung, L. Stryer, Surface density determination in membranes by fluorescence energy transfer, Biochemistry 17 (1978) 5241–5248.
[23] S.G. Peisajovich, O. Samuel, Y. Shai, Paramyxovirus F1 protein has two fusion peptides: implications for the mechanism of membrane fusion, J. Mol. Biol. 296 (2000) 1353–1365.
[24] D.K. Chang, W.J. Chien, S.F. Cheng, The FLG motif in the N-terminal region of glycoprotein 41 of human immunodeficiency virus type 1 adopts a type I (-turn in aqueous solution and serves as the initiation site for helix formation, Eur. J. Biochem. 247 (1997) 896–905.
[25] D.C. Rees, L. DeAntonio, D. Eisenberg, Hydrophobic organization of membrane proteins, Science 245 (1989) 510–513.
[26] B.D. Adair, D.M. Engelman, Glycophorin A helical transmembrane domains dimerize in phospholipid bilayers: a resonance energy transfer study, Biochemistry 33 (1994) 5539–5544.
[27] D.Z. Cleverley, J. Lenard, The transmembrane domain in viral fusion: essential role for a conserved glycine residue in vesicular stomatitis virus G protein, Proc. Natl. Acad. Sci. U. S. A. 95 (1998) 3425–3430.
[28] M.S. Weiss, A. Kreusch, E. Schiltz, U. Nestel, W. Welte, J. Wekesser, G.E. Schulz, The structure of porin from *Rhodobacter capsulatus* at 1.8 Å resolution, FEBS Lett. 280 (1991) 379–382.
[29] C.I. Bargmann, R.A. Weinberg, Oncogenic activation of the neu-encoded receptor protein by point mutation and deletion, EMBO J. 7 (1988) 2043–2052.
[30] A. Bundi, K. Wüthrich, ^{1}H NMR titration shifts of amide proton resonances in polypeptide chains, FEBS Lett. 77 (1977) 11–14.
[31] A. Leo, C. Hansch, D. Elk, Partition coefficients and their uses, Chem. Rev. 71 (1971) 525–616.
[32] X. Han, J.H. Bushweller, D.S. Cafiso, L.K. Tamm, Membrane structure and fusion-triggering conformational change of the fusion domain from influenza hemagglutinin, Nat. Struct. Biol. 8 (2001) 715–720.
[33] A. Bundi, K. Wüthrich, Use of amide ^{1}H-nmr titration shifts for studies of polypeptide conformation, Biopolymers 18 (1979) 299–311.
[34] M. Eilers, S.C. Shekar, T. Shieh, S.O. Smith, P.J. Fleming, Internal packing of helical membrane proteins, Proc. Natl. Acad. Sci. 97 (2000) 5796–5801.
[35] X. Han, L.K. Tamm, pH-dependent self-association of influenza hemagglutinin fusion peptides in lipid bilayers, J. Mol. Biol. 304 (2000) 953–965.
[36] I.A. Wilson, J.J. Skehel, D.C. Wiley, Structure of the hemaegglutinin membrane glycoprotein of influenza virus at 3 Å resolution, Nature 28 (1981) 368–373.
[37] S.T. Russell, A. Warshel, Calculations of electrostatic energies in proteins. The energetics of ionized groups in bovine pancreatic trypsin inhibitor, J. Mol. Biol. 185 (1985) 389–404.
[38] K. Langsetmo, J.A. Fuchs, C. Woodward, The conserved, buried aspartic acid in oxidized *Escherichia coli* thioredoxin has a pKa of 7.5. Its titration produces a related shift in global stability, Biochemistry 30 (1991) 7603–7609.
[39] S. Lew, J. Ren, E. London, The effects of polar and/or ionizable residues in the core and flanking regions of hydrophobic helices on transmembrane conformation and oligomerization, Biochemistry 39 (2000) 9632–9640.
[40] K. Kasahara, Y. Nakayama, K. Ikeda, Y. Fukushima, D. Matsuda, S. Horimoto, N. Yamaguchi, Trafficking of Lyn through the Golgi caveolin involves the charged residues on (E and (I helices in the kinase domain, J. Cell Biol. 165 (2004) 641–652.
[41] A.W. Patridge, R.A. Melnyk, C.M. Deber, Polar residues in membrane domain of proteins: molecular basis for helix–helix association in a mutant CFTR transmembrane segment, Biochemistry 41 (2002) 3647–3653.
[42] H. Gratkowski, J.D. Lear, W.F. DeGrado, Polar side chains drive the association of model transmembrane peptides, Proc. Natl. Acad. Sci. U. S. A. 98 (2001) 880–885.
[43] F.X. Zhou, H.J. Merianos, A.T. Brunger, D.M. Engelman, Polar residues drive association of polyleucine transmembrane helices, Proc. Natl. Acad. Sci. U. S. A. 98 (2001) 2250–2255.
[44] G.A. Caputo, E. London, Position and ionization state of Asp in the core of membrane-inserted α-helices control both the equilibrium between transmembrane and nontransmembrane helix topography and transmembrane helix positioning, Biochemistry 43 (2004) 8794–8806.
[45] M. Monné, I. Nilsson, M. Johansson, N. Elmhed, G. von Heijne, Positively and negatively charged residues have different effects on the position in the membrane of a model transmembrane helix, J. Mol. Biol. 284 (1998) 1177–1183.
[46] J.L. Popot, D.M. Engelman, Helical membrane protein folding, stability, and evolution, Annu. Rev. Biochem. 69 (2000) 881–922.
[47] H. Belrhali, P. Nollert, A. Royant, C. Menzel, J.P. Rosenbusch, E.M. Landau, Protein, lipid and water organization in bacteriorhodopsin crystals: a molecular view of the purple membrane at 1.9 Angstrom resolution, Structure 7 (1999) 909–917.
[48] J.D. Jones, L.M. Gierasch, Effect of charged residue substitution on the membrane-interactive properties of signal sequences of the *Escherichia coli* LamB protein, Biophys. J. 67 (1994) 1534–1545.
[49] M. Sundaralingam, Y.C. Sekharudu, Water-inserted α-helical segments implicate reverse turns as folding intermediates, Science 244 (1989) 1333–1337.
[50] P.Y.S. Lam, P.K. Jadhav, C.J. Eyerman, C.N. Hodge, Y. Ru, L.T. Bacheler, J.L. Meek, M.J. Otto, M.M. Rayner, Y.N. Wong, C.H. Chang, P.C. Weber, D.A. Jackson, T.R. Sharpe, S. Erickson-Viietanen, Rational design of potent, bioavailable, nonpeptide cyclic ureas as HIV protease inhibitors, Science 263 (1994) 380–384.
[51] D.A. Doyle, J.M. Cabral, R.A. Pfuetzner, A. Kuo, J.M. Gulbis, S.L. Cohen, B.T. Chait, R. MacKinnon, The structure of the potassium channel: molecular basis of K^{+} conduction and selectivity, Science 280 (1998) 69–77.
[52] A.R. Walmsley, M.P. Barrett, F. Bringaud, G.W. Gould, Sugar transporters from bacteria, parasites and mammals: structure–activity relationships, Trends Biochem. Sci. 23 (1998) 476–481.